

Zbigniew Pędzich¹, Robert Jasionowski², Magdalena Ziąbka¹

¹ AGH - University of Science and Technology, Faculty of Materials Science and Ceramics, Department of Ceramics and Refractory Materials
al. Mickiewicza 30, 30-059 Krakow, Poland

² Maritime Academy, Institute of Basic Technical Sciences, Department of Shipbuilding Materials Engineering, ul. Podgórna 51-53, 70-506 Szczecin, Poland

*Corresponding author. E-mail: pedzich@agh.edu.pl

Received (Otrzymano) 5.08.2014

CAVITATION WEAR OF CERAMICS - PART II. CAVITATION WEAR MECHANISMS OF COMPOSITES WITH OXIDE MATRICES

The usage of ceramic materials in applications endangered by intensive cavitation could limit erosion phenomena. Especially effective improvement could be achieved with the application of sintered ceramic matrix composites (CMC). The presented work describes the cavitation wear resistance of a few CMCs in comparison to mono-phase ceramic sinters made of alumina and tetragonal zirconia. Their degradation was described by the volumetric loss of material. Additionally, the cavitation degradation mechanisms of each particular material were determined by detailed observations of worn surfaces at different stages of wear.

Keywords: cavitation, erosion, ceramic matrix composites

ZUŻYCIE KAWITACYJNE CERAMIKI - CZĘŚĆ II. MECHANIZMY ZUŻYCIA KAWITACYJNEGO KOMPOZYTÓW NA OSNOWACH TLENKOWYCH

Użycie materiałów ceramicznych w zastosowaniach, w których materiał narażony jest na intensywną kawitację, może ograniczyć zużycie. Szczególnie efektywną poprawę można uzyskać, stosując spieki kompozytów ziarnistych składające się z faz ceramicznych (CMC). Prezentowana praca przedstawia odporność na zużycie kawitacyjne kilku materiałów kompozytowych w odniesieniu do jednofazowych spieków tlenkowych (korundu oraz tetragonalnych polikryształów dwutlenku cyrkonu). Porównane zostały wartości zużycia objętościowego oraz mechanizmy zniszczenia poszczególnych materiałów. Te ostatnie określano poprzez szczegółową obserwację stanu powierzchni na różnych etapach zużycia.

Słowa kluczowe: kawitacja, erozja, kompozyty z osnową ceramiczną

INTRODUCTION

Cavitation is a phenomenon caused by the repeated nucleation, growth, and violent collapse of clouds of bubbles within a liquid. Microstreams of liquid developed during the implosion of cavitation bubbles as well as the action of pressure waves from disappearing bubbles are the main causes of destruction on swilled surfaces leading to a loss of material, i.e. to cavitation erosion. On the surface of material exposed to the actions of liquids, the cavitation phenomenon induces local destruction of the surface layer as a consequence of the resultant effect of liquid micro-stream blows with high hydrodynamic parameters as well as pressure waves. Due to the loading nature, the destruction of the material surface can be compared to the fatigue process [1-3]. This means that materials with a greater resistance to cavitation erosion are first of all characterised by high hardness and micro-hardness as well as a fine-

grained one-phase microstructure having internal compressive stresses [4-6].

The use of ceramic materials in applications endangered by intensive cavitation could limit corrosion phenomena. The number of works devoted to the investigation of resistance to cavitation erosion of ceramic materials is not large [7-12] and they concern the properties of pure phases, such as alumina, zirconia, silicon nitride or some glass types. As a result, the mentioned works have given some useful data suggesting which phases could be more resistant than others and how the microstructure of sinters could influence ceramic phases susceptibility to cavitation wear. Some observations concerning the cavitation wear of ceramic composites were described in [13]. The presented work is a continuation of the investigations described in [14]. It reports investigations of cavitation erosion resistance

for a few ceramic composites based on α -alumina and tetragonal zirconia matrices.

EXPERIMENTAL PROCEDURE

Cavitation wear investigations were conducted for six types of ceramic sinters. Two of them were commonly used oxide materials: α -alumina and tetragonal zirconia. For sinters fabrication, commercial powders were applied: Al_2O_3 - TM-DAR, produced by Taimicron Inc. (Japan), and yttria stabilized ZrO_2 powder 3Y-TZ, produced by Tosoh (Japan). These materials are indicated in this work as **A** and **Z**, for alumina and zirconia, respectively.

The other investigated materials were composites. Two materials based on an alumina matrix and two others based on a tetragonal zirconia matrix. Each composite contains 10 vol.% second phase particles. In the case of the alumina matrix composite, the tetragonal zirconia (3Y-TZ) and yttria-alumina garnet particles (YAG) (non-commercial manufacturing method was described in [15]) were introduced. In the case of the zirconia matrix composite, alumina (TM-DAR) and tungsten carbide particles (Baildonit, Poland) were added.

The composite materials for the investigations are indicated in this work as follows: **AZ**, **AY**, **ZA** and **ZW** for the alumina/zirconia, alumina/YAG, zirconia/alumina and zirconia/carbide composites, respectively.

These materials were selected due to previous works [16, 17] as materials showing good mechanical properties, particularly in wear tests. Most of the sinters were fabricated in an uncomplicated way. The composite powders were produced by mixing the constituent powders in attritor mill in ethyl alcohol and dried. Only the **AY** material was manufactured by a different chemical method described in detail in [15]. The samples were uni-axially pressed under 50 MPa, consequently iso-statically re-pressed under 300 MPa and then pressureless sintered at 1500°C (for **A**, **AZ** and **AY**) or 1550°C (for **Z** and **ZA**). The dwell time of 2 hours was the same

for all the mentioned samples. The only samples prepared by the hot-pressing technique were made of **ZW**. The sintering process was conducted under 25 MPa at 1600°C with a 1 h dwell time in an argon atmosphere.

The relative density of the materials was calculated as a quotient of the apparent and theoretical density. The apparent density of the materials was measured by the Archimedes method. The theoretical density for alumina was 3.99 g/cm³, for the applied zirconia material 6.1 g/cm³ and for tungsten carbide 15.7 g/cm³ (according to producers data). The YAG theoretical density of 4.56 g/cm³ was received according to [18].

The hardness (*HV*) and fracture toughness (*K_{IC}*) were measured by the Vicker's indentation method, based on the Niihara calculation model [19], using Nanotech MV-700 equipment. The load was 49.05 N for the hardness measurements and 98.1 N for the *K_{IC}* calculations. The data for the strength analysis were collected from three-point bending tests conducted on 30 x 2.5 x 2 mm bars. Selected sinter parameters are presented in Table 1.

The examination of cavitation erosion was carried out on a jet-impact device described in detail in [20]. The samples for the examination were of cylindrical shape, 20 mm in diameter and 6 ±0.5 mm in height. The sample surface roughness, measured by means of a PGM-1C profilometer, was about 0.03 μm. The samples were mounted vertically on rotor arms, parallel to the axis of water stream pumped continuously at 0.06 MPa through a nozzle with a 10 mm diameter, 1.6 mm away from the sample edge. The rotating samples were struck with the water stream. The water flow intensity was constant and amounted to 1.55 m³/h. The wear rate was determined by sample weighing up to the total time of 2400 minutes. The volumetric wear rate was calculated as a quotient of weight loss and apparent density of each investigated sample. Calculations were performed after 500, 900, 1200, 1500, 1800, 2400 and 3000 minutes of testing. The worn material surfaces were observed by means of the SEM technique with a FEI NOVA NANO 200 device.

TABLE 1. Selected properties of investigated ceramic sinters
TABELA 1. Wybrane właściwości badanych spieków ceramicznych

Material	Apparent density [g/cm ³]	Relative density % of theo.	Vicker's hardness <i>HV₅</i> [GPa]	Young's modulus <i>E</i> [GPa]	Fracture toughness <i>K_{IC}</i> [MPam ^{0.5}]	Bending strength σ [MPa]
Al_2O_3	3.96 ±0.1	99.3	17.0 ±1.2	379 ±6	3.6 ±0.3	600 ±120
ZrO_2	6.07 ±0.1	99.5	14.0 ±0.5	209 ±5	5.0 ±0.5	1150 ±55
$\text{Al}_2\text{O}_3/\text{ZrO}_2$	4.14 ±0.1	98.5	17.0 ±0.4	361 ±5	5.1 ±0.5	800 ±120
Al_2O_3 -YAG	4.01 ±0.1	98.9	19.0 ±1.1	370 ±8	6.0 ±0.7	580 ±45
ZrO_2/WC	7.04 ±0.1	99.7	17.0 ±0.9	232 ±6	8.0 ±1.0	1100 ±130
$\text{ZrO}_2/\text{Al}_2\text{O}_3$	5.89 ±0.1	99.0	15.0 ±0.6	216 ±4	6.0 ±0.4	1050 ±55

RESULTS AND DISCUSSION

The basic results of the test are collected in Figure 1. It presents the volumetric wear of the investigated materials during the stream impact test.

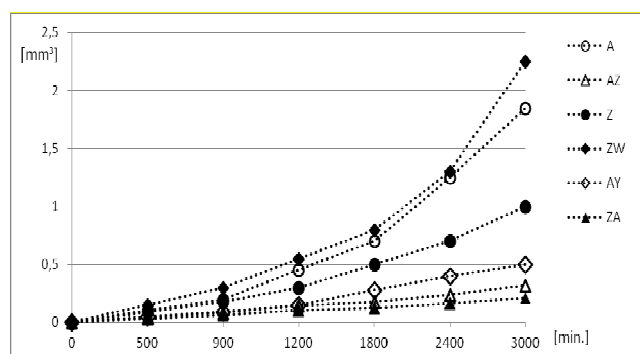


Fig. 1. Volumetric wear of investigated materials during stream impact test

Rys. 1. Zużycie objętościowe materiałów badanych podczas testu strumieniowo-uderzeniowego

As can be easily recognized, all the materials composed of oxide phases only showed cavitation wear resistance much better than the mono-phase materials.

Only in the case of the **ZW** composite, a worse result was registered.

Figure 2 illustrates the state of the **AY** material surface before (Fig. 2a) and after 1200 min. of cavitation testing (Fig. 2b), observed by means of the SEM technique. It is distinctly visible that in that case, the YAG particles were very uniformly distributed in the alumina matrix. The material loss took place only by the removal of small individual particles. Even after a long duration of the test (Fig. 3a), this mechanism did not change. This degradation mechanism is similar to the pure alumina (**A**) material (Fig. 3b) but in that case, the individual grains were bigger and the each single act of volume loss was more destructive [14]. The microstructure observation of the **AZ** material (Fig. 4a) showed that the uniformity of the additive grains distribution was worse than in the **AY** material. A few micrometer large alumina grains could be detected among the well-homogenized areas. As is clearly visible in Figure 4b, the first acts of degradation started in these larger alumina agglomerates. The consequence of these voids was greater degradation localised around primary holes (Fig. 5). It is worth noticing that in the end, the **AZ** material was better than **AY** after 3000 mins of wear testing.

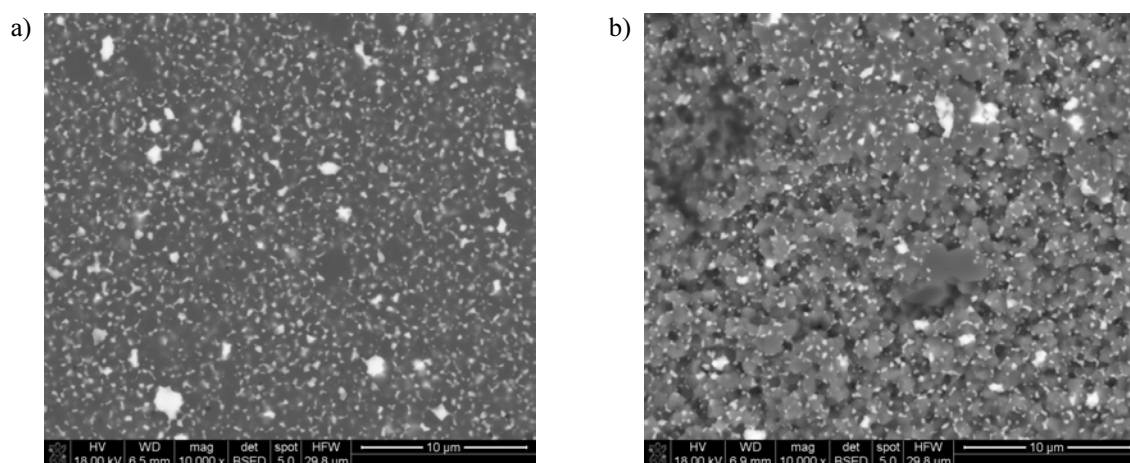


Fig. 2. SEM images of AY material before (a) and after 1200 min (b) of cavitation testing

Rys. 2. Obrazy SEM materiału AY przed (a) i po 1200 min (b) testu kawitacyjnego

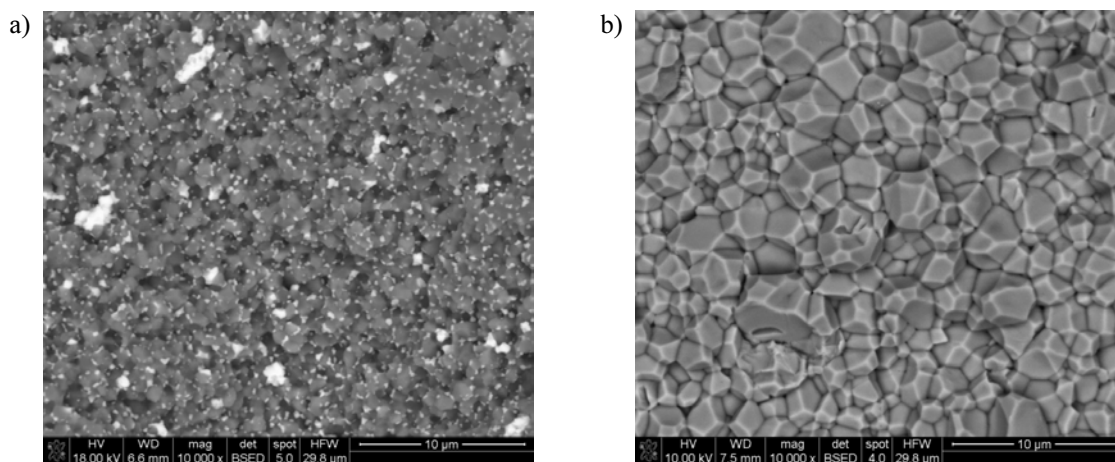


Fig. 3. SEM images of AY (a) and A (b) materials after 2400 min of cavitation testing

Rys. 3. Obrazy SEM dla AY (a) i A (b) po 2400 min testu kawitacyjnego

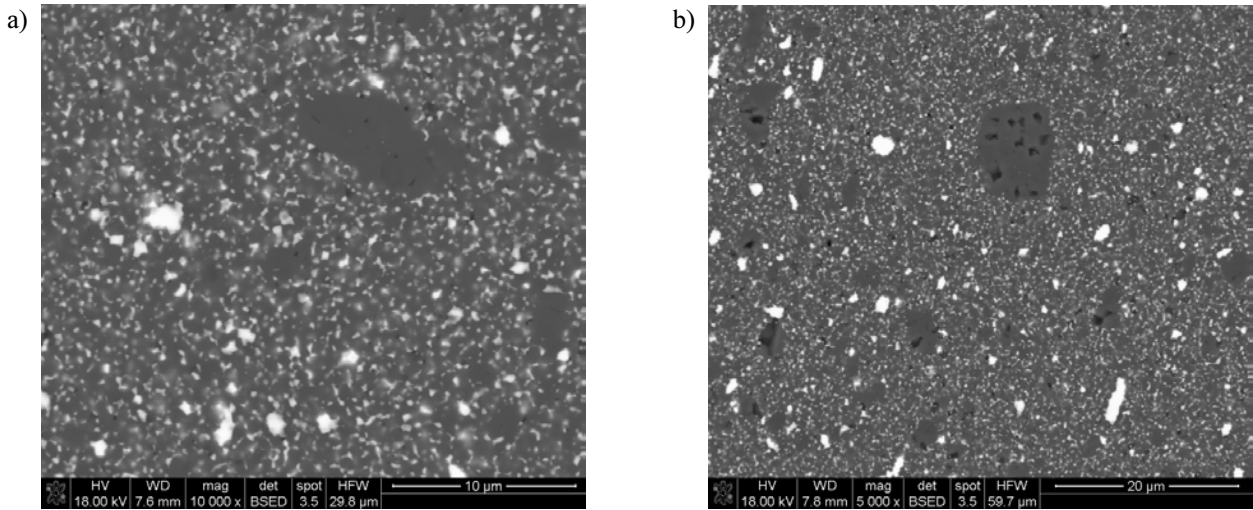


Fig. 4. SEM images of AZ material before (a) and after 1200 min (b) of cavitation testing

Rys. 4. Obrazy SEM materiału AZ przed (a) i po 1200 min (b) testu kawitacyjnego

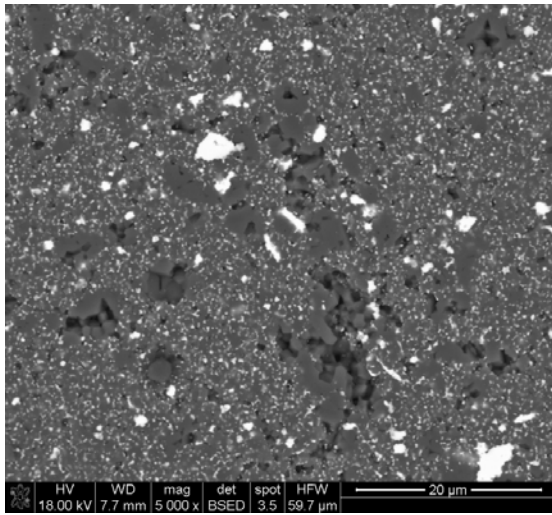


Fig. 5. SEM image of AZ material after 2400 min of cavitation testing

Rys. 5. Obraz SEM materiału AZ po 2400 min testu kawitacyjnego

The best cavitation wear resistance was shown by the **ZA** composite. This material as visible in the SEM images (Fig. 6a) has the best homogenisation of the dispersed second phase (alumina) among all the investigated composites. The second measurements of wear rate, performed after 1200 mins, showed very limited, first stage degradation (Fig. 6b). The wear mechanism of the **ZA** degradation (Fig. 7a) was similar to the mechanism of the pure zirconia (**Z**) degradation described in [14] and illustrated in Figure 7b.

The worst cavitation wear resistance was shown by the **ZW** composite. The SEM images analysis gave the answer to the question: why does the best densified material with excellent mechanical properties have poor cavitation wear resistance? Most probably, the agglomeration of fine carbide inclusions visible in Figures 8a-b was easily destroyed by the intensive cavitation load. The removal of whole carbide agglomerates resulted in fast material degradation.

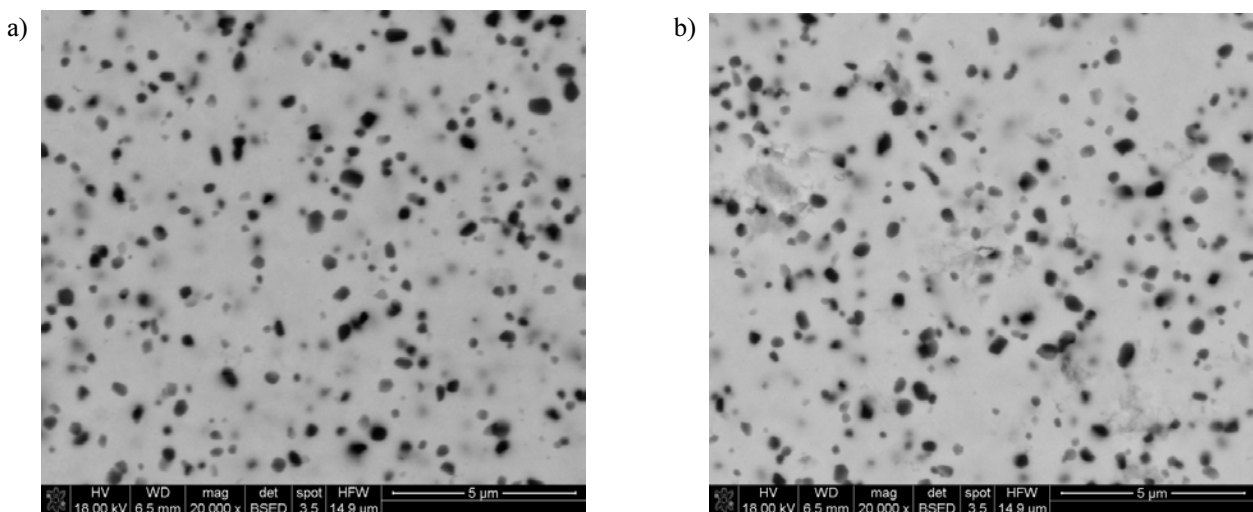


Fig. 6. SEM images of ZA material before (a) and after 1200 min (b) of cavitation testing

Rys. 6. Obrazy SEM materiału ZA przed (a) i po 1200 min (b) testu kawitacyjnego

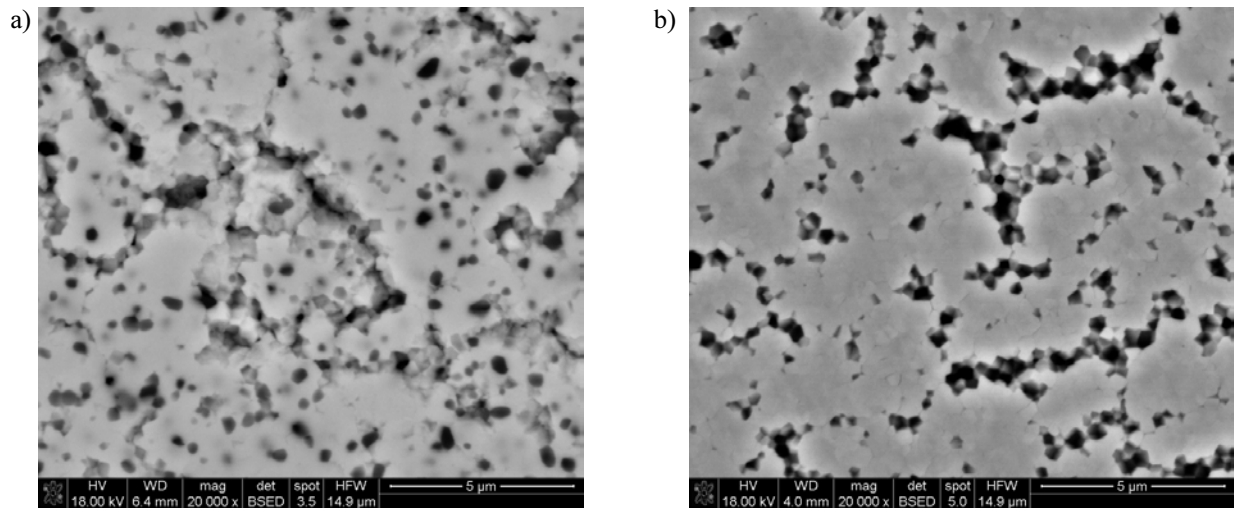


Fig. 7. SEM images of ZA (a) and A (b) materials after 2400 min of cavitation testing

Rys. 7. Obrazy SEM dla ZA (a) i Z (b) po 2400 min testu kawitacyjnego

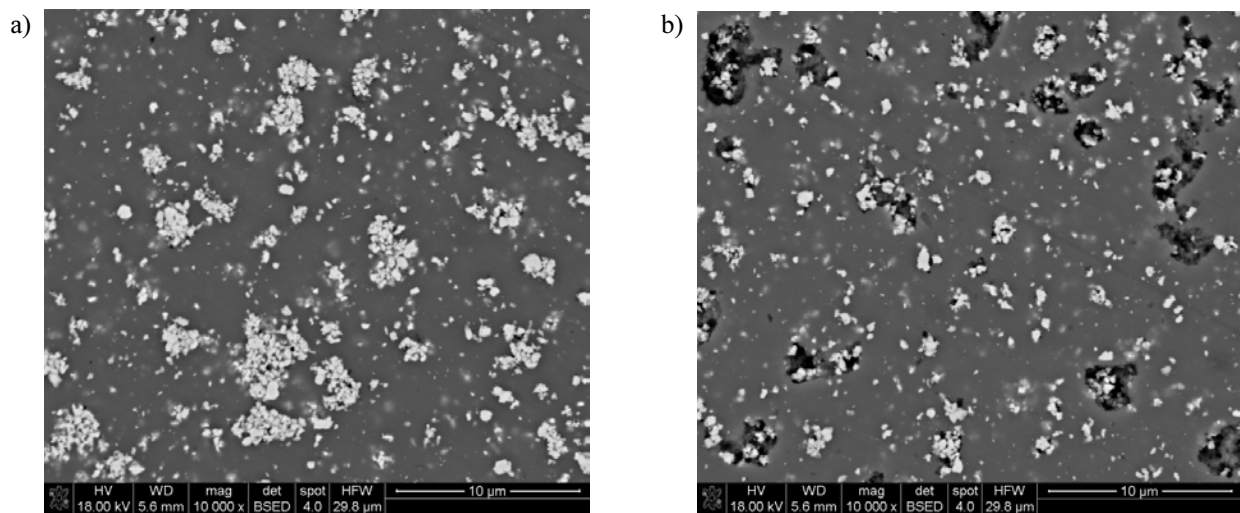


Fig. 8. SEM images of ZW material before (a) and after 600 min (b) of cavitation testing

Rys. 8. Obrazy SEM materiału ZW przed (a) i po 1200 min (b) testu kawitacyjnego

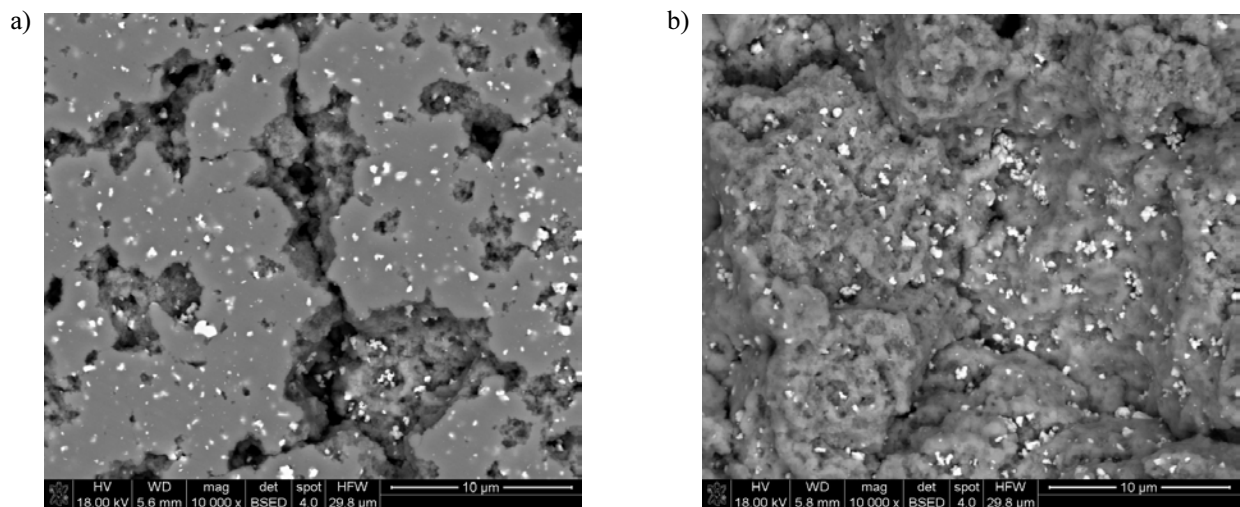


Fig. 9. SEM images of ZW material after 1200 (a) and 2400 min (b) of cavitation testing

Rys. 9. Obrazy SEM materiału ZW po 1200 (a) i 2400 min (b) testu kawitacyjnego

It is commonly known that in sintered CMC materials, residual stress caused by differences in the thermal expansion (α) coefficient values of the constituent phases are present. For the phases used in the present investigations, the α coefficients were as follows: $\alpha_{\text{ZrO}_2} = 11.0 \cdot 10^{-6} \text{C}^{-1}$, $\alpha_{\text{Al}_2\text{O}_3} = 9.2 \cdot 10^{-6} \text{C}^{-1}$, $\alpha_{\text{YAG}} = 9.1 \cdot 10^{-6} \text{C}^{-1}$ and $\alpha_{\text{WC}} = 5.2 \cdot 10^{-6} \text{C}^{-1}$. Theoretically [21], the rule is that relation $\alpha_{\text{matrix}} < \alpha_{\text{inclusion}}$ results in tension stresses in the matrix, which should act as an additional toughening mechanism for the material. The opposite relation $\alpha_{\text{matrix}} > \alpha_{\text{inclusion}}$ should weaken the composite. Short analysis of the data indicates that toughening by residual stresses should be expected for the **AZ** material [22]. The opposite effect should be noticed for the **ZA** and **ZW** materials. For the **AY** composite, the difference in the α coefficients was too small to significantly influence the stress distribution. Analysis of the results presented in Figure 1 suggest that the residual stresses were not decisive in the wear resistance of the investigated materials. The **ZA** material with non-profitable residual stress distribution had the best cavitation wear resistance. It seems that the microstructural factors were much more important for the composite properties.

SUMMARY

The performed tests ranked the investigated materials regarding their cavitation wear resistance. The results of volumetric wear and analysis of the worn surfaces microstructure indicated that the investigated materials did not have comparable microstructures. It is worth noticing that a similar method of composite preparation led to microstructural differences due to the different physicochemical properties of the initial powders. As indicated, such differences could influence the cavitation wear process. The general conclusion is that the most promising properties were demonstrated by the composites composed of zirconia and alumina. The best results were achieved by the **ZA** and **AZ** materials. The results achieved during the performed tests suggest that the microstructural factor is more important for wear resistance than the residual stress distribution in composites.

Acknowledgements

The research has been funded by the Polish Ministry of Education and Science as AGH - University project no. 11.11.160.617.

REFERENCES

- [1] Brennen C.E., Cavitation and Bubble Dynamics, Oxford University Press, 1995.
- [2] Briggs L.J., The limiting negative pressure of water, Journal of Applied Physics, 21, 1970, 721-722.
- [3] Trevena D.H., Cavitation and Tension in Liquids, IOP Publishing Ltd, 1987.
- [4] Plesset M.S., Chapman R.B., Collapse of an Initially spherical vapour cavity in the neighbourhood of a solid boundary, Jour. Fluid Mech. 1971, 47 (2), 283-290.
- [5] Hickling R., Plesset M.S., Collapse and rebound of a spherical bubble in water, Phys. Fluids 1963, (7), 7-14.
- [6] Naude C.F., Ellis A.T., On the mechanism of cavitation damage by non-hemispherical cavities collapsing in contact with a solid boundary, Journal of Basic Engineering 1961, 83, 648-656.
- [7] Tomlinson W.J., Matthews S.J., Cavitation erosion of structural ceramics, Ceramics International 1994, 20 (3), 201-209.
- [8] Tomlinson W.J., Kalitsounakis N., Vekinis G., Cavitation erosion of aluminas, Ceramics International 1999, 25 (4), 331-338.
- [9] Niebuhr D., Cavitation erosion behavior of ceramics in aqueous solutions, Wear 2007, 263(1-6), 295-300.
- [10] Garcia-Atance Fatjo G., Hadfield M., Tabeshfar K., Pseudoplastic deformation pits on polished ceramics due to cavitation erosion, Ceramics International 2011, 37, 1919-1927.
- [11] Lua J., Zum Gahr K.-H., Schneider J., Microstructural effects on the resistance to cavitation erosion of ZrO₂ ceramics in water, Wear 2008, 265, 1680-1686.
- [12] Pędzich Z., Jasionowski R., Lach R., Przetakiewicz W., Cavitation Resistance of Sintered Alumina and Composites on Its Base, [in:] Innovative Manufacturing Technology 2, Ed. P. Rusek, Institute of Advanced Manufacturing Technology, Krakow 2012, 393-402.
- [13] Pędzich Z., Jasionowski K., Ziabka M., Cavitation wear of structural oxide ceramics and selected composite materials, J. Eur. Ceram. Soc. 2014, 34(14), 3351-56.
- [14] Pędzich Z., Jasionowski R., Ziabka M., Cavitation wear of ceramics - part I. Mechanisms of cavitation wear of alumina and tetragonal zirconia sintered polycrystals, Composites Theory and Practice 2013, 13(4), 288-292.
- [15] Lach R., Haberko K., Bućko M.M., Szumera M., Grabowski G., Ceramic matrix composites in the alumina/5-30 vol.% YAG system, J. Eur. Ceram. Soc. 2011, 31, 1889-1895.
- [16] Pędzich Z., The abrasive wear of alumina matrix particulate composites at different environments of work, [in:] D. Zhang, K. Pickering, B. Gabbitas, P. Cao, A. Langdon, R. Torrens, et al., editors, Advanced Materials and Processing IV, vol. 29-30, Switzerland, Trans Tech Publications, 2007, 283-286.
- [17] Pędzich Z., Zużycie abrazyjne kompozytów ziarnistych na osnowach tlenkowych, Kompozyty/Composites 2008, 8(4), 403-408.
- [18] Lach R., Haberko K., Trybalska B., Composite material in the Al₂O₃-20 vol% YAG system, Processing and Application of Ceramics 2010, 4(1), 1-6.
- [19] Niihara K., A fracture mechanics analysis of indentation, J. Mater. Sci. Lett. 1983, 2, 221-223.
- [20] Jasionowski R., Przetakiewicz W., Zasada D., The effect of structure on the cavitation wear of FeAl intermetallic phase-based alloys with cubic lattice, Archives of Foundry Engineering 2011, 11, Special Issue 2, 97-102.
- [21] Taya M., Hayashi S., Kobayashi A.S., Yoon H.S., Toughening of a particulate-reinforced ceramic-matrix composite by thermal residual stress, J. Amer. Ceram. Soc. 1990, 73(5) 1382-1391.
- [22] Grabowski G., Pędzich Z., Residual stresses in particulate composites with alumina and zirconia matrices, J. Europ. Ceram. Soc. 2007, 27(2-3), 1287-1292.

